UNDERWATER SHEAR-STRESS SENSOR

Yong Xu, Fukang Jiang[*], Qiao Lin[**], Jason Clendenen[***], Steve Tung[***] and Yu-Chong Tai
California Institute of Technology, Pasadena, USA
[*]Umachines Inc., Pasadena, USA
[**]Carnegie Mellon University, Pittsburgh, USA
[***]University of Arkansas, Fayetteville, USA

ABSTRACT

This paper reports the development of a micromachined, vacuum-cavity insulated, thermal shear-stress sensor for underwater applications. This paper is focused on the two major challenges for underwater shear-stress sensors: the waterproof coating and pressure sensitivity. It is found that thin-film CVD Parylene is a good waterproof material and sensors coated with 2 μm Parylene N can survive in water for at least one month at 55 °C. It is also found that reducing the size and increasing the thickness of the sensor diaphragm are effective in minimizing the pressure sensitivity.

INTRODUCTION

Wall shear stress measurement is of crucial importance for a lot of fluid dynamic monitoring and diagnostics applications. For example, we have developed shear-stress sensors for the flow separation detection for an unmanned aerial vehicle [1] and for active drag reduction [2]. Interestingly, however, most the MEMS effort so far has been mainly spent on developing sensors in air, rather than in liquid (e.g., water) [3-6]. At the same time, there are a lot of underwater applications that require shear-stress sensors. Examples include the flow field measurement of radio-controlled submarines and the safety and arming device of torpedoes. However, there is a lack of underwater shear-stress sensor from the market.

It is then the purpose of this work to develop a vacuum-cavity insulated thermal shear-stress sensor for underwater applications. As shown in Figure 1, the basic structure of the sensor is a polysilicon resistor sitting on a nitride diaphragm with a vacuum cavity underneath, which provides excellent thermal isolation to reduce the heat loss to substrate. In this design, the input power of the resistor will change with the wall shear stress from the ambient flow field and this change can be readily detected electronically.

This design is actually based on our aerial shear-stress sensor [3, 4]. However, there are two major challenges when modifying the aerial design for underwater applications. The first challenge is to develop a compatible waterproof coating to enable the sensor to operate under water for long enough time (e.g., one month is the goal for this work). The second challenge is to minimize the crosstalk from the sensors' pressure sensitivity. This usually is not a serious problem for aerial application since the air pressure does not vary a lot in most applications. However, the water pressure exerted on the sensor can change significantly such as during a submarine dive. Therefore, these two issues are the main foci of the study.
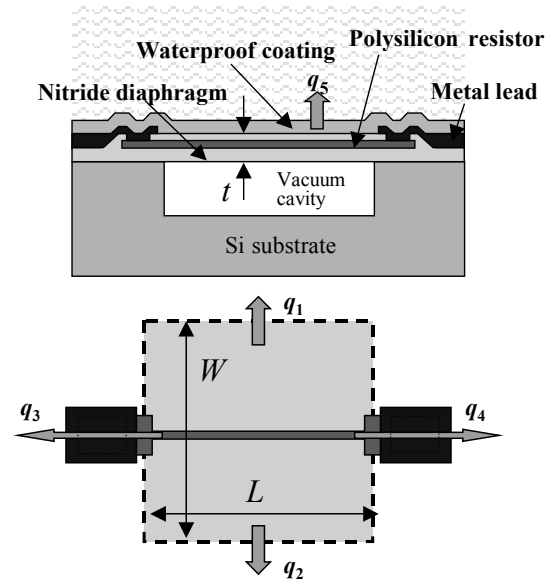

Figure 1 The cross section and top view of the underwater shear-stress sensor.

WATERPROOF COATING

For waterproof coating, low temperature oxide (LTO) was originally investigated, but then quickly abandoned because the sensor will be integrated onto a flexible skin eventually for packaging purpose [1] and tests show that LTO cracks easily to destroy the devices. Parylene was then investigated and concluded to be an adequate waterproof material. Here, Parylene is the generic name for members of unique family of thermoplastic polymers that are deposited by using the dimer of para-xylylene (di-para-xylylene, or DPXN). It is flexible, resistant to water permeation, and easily CVD-deposited at room temperature. Table 1 compares the moisture vapor transmission rates of Parylene N, C, D (which are the 3 most frequently used types of Parylene) and other polymers [7].

Underwater tests show that, when operated at 55 °C, sensors coated with 2 μm Parylene N can survive in water for at least one month. Longer survival time is expected with Parylene C, which has a much smaller moisture transmission rate.

Table 1 Moisture transmission rates of different polymers.

Polymer	Moisture Vapor Transmission at 90% RH, 37 °C, (g•mil/100 in^2•d)
Parylene N	1.5
Parylene C	0.21
Parylene D	0.25
Epoxides	1.79 - 2.38
Silicones	4.4 - 7.9
Urethanes	2.4 – 8.7

PRESSURE SENSITIVITY

For the polysilicon resistor across the diaphragm (Figure 1), the resistance change caused by pressure can be expressed as

$$\Delta R / R = G_l \overline{\varepsilon_l} + G_t \overline{\varepsilon_t} \qquad (1)$$

$\overline{\varepsilon_l}$:   averaged longitudinal strain

$\overline{\varepsilon_t}$:   averaged transverse strain

G_l: longitudinal gauge factor of polysilicon
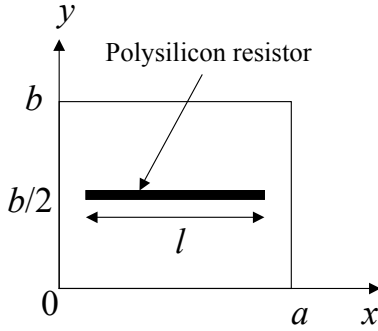
G_t: transverse gauge factor of polysilicon

Figure 2 The coordinate axes.

Unfortunately, the strain distribution calculation is a challenging problem due to the step-up anchor and bird's beak of the diaphragm [8]. Moreover, the intrinsic stress of SiN makes the problem even more complicated. If we assume the diaphragm is an ideal flat plate with clamped edge boundary and zero initial stress, an analytical approximation of strain distributions at both x and y directions can be obtained [9] using the coordinate axes shown in Figure 2:

$$\varepsilon_x(x,y) = \frac{2\pi^2 t}{a^2} \sum_{m=1}^{\infty}\sum_{n=1}^{\infty} A_{mn} m^2 \cos\frac{2m\pi x}{a}(1-\cos\frac{2n\pi y}{b}) \qquad (2)$$

$$\varepsilon_y(x,y) = \frac{2\pi^2 t}{b^2} \sum_{m=1}^{\infty}\sum_{n=1}^{\infty} A_{mn} n^2 \cos\frac{2n\pi y}{b}(1-\cos\frac{2m\pi x}{a}) \qquad (3)$$

where t is the thickness of the plate and A_{mn} are the coefficients which can be determined by Rayleigh-Ritz method. The average strains can then be expressed as

$$\overline{\varepsilon_l} = \frac{1}{l} \int_{(a-l)/2}^{(a+l)/2} \varepsilon_x(x,y)\Big|_{y=0.5b} dx \qquad (4)$$

$$\overline{\varepsilon_t} = \frac{1}{l} \int_{(a-l)/2}^{(a+l)/2} \varepsilon_y(x,y)\Big|_{y=0.5b} dx \qquad (5)$$

Based on Equation (1-5), the theoretical resistance change can be calculated as a function of the resistor length. It is found that the longitudinal and transverse terms of Equation (1) can be fully compensated at some certain resistor length. Namely, the pressure sensitivity could be completely eliminated with any diaphragm size if the sensing element is properly placed.

However, the reality is much more complicated. Figure 3 shows the measured pressure sensitivity data of 4 identical aerial shear-stress sensors with square diaphragms 210 μm wide and 1.6 μm thick. These 4 sensors, which have identical parameters such as diaphragm dimension and resistor length, were expected to have the same characteristics. However, as shown in Figure 3, their pressure sensitivities vary considerably. There are a lot of factors contributing to the large fluctuation of the pressure sensitivities. Among them, the dimension of the diaphragm is believed to play a key role.
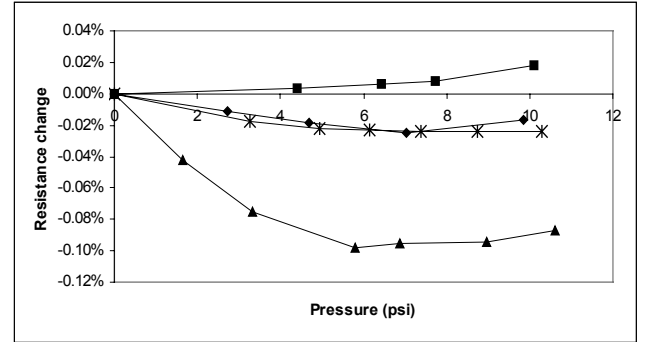

Figure 3 Pressure sensitivity of four aerial shear-stress sensors.

In this work, we then choose to employ smaller and thicker diaphragms to minimize the pressure sensitivity. The biggest benefit by doing this is that, the uncompensated strain, due to the model error or imperfect process control (e.g., the resistor position offset), will be significantly reduced with a stiffer diaphragm. Moreover, the touchdown of the diaphragm will happen at much higher pressure so that the operation range of the shear-stress sensor can be extended considerably. The drawbacks, of course, are more conductive heat loss to substrate and smaller shear-stress sensitivity.

DESIGN AND FABRICATION

As a result, we have miniaturized the diaphragm sides and increased thickness of our sensors for underwater applications. In order to perform a comparative study, sensors with different diaphragm dimensions are implemented. We keep the length, L, a constant (210 μm), but the width, W, varies as 210 μm, 150 μm, 100 μm, 75 μm, and 45 μm. For all the designs,

the thickness is chosen as 4 μm in order to make the diaphragm rigid enough but not to cause any difficult problem in the fabrication process. A temperature sensor is integrated for temperature compensation while a pressure sensor is also included in case pressure compensation is needed.

1. Deposit and pattern nitride.

2. Local oxidation. Deposit and pattern PSG.

3. Deposit nitride and open etching holes.

4. Remove oxide and PSG. Deposit nitride.

5. Deposit, dope and pattern polysilicon.

6. Deposit nitride passivation layer and Al metallization.
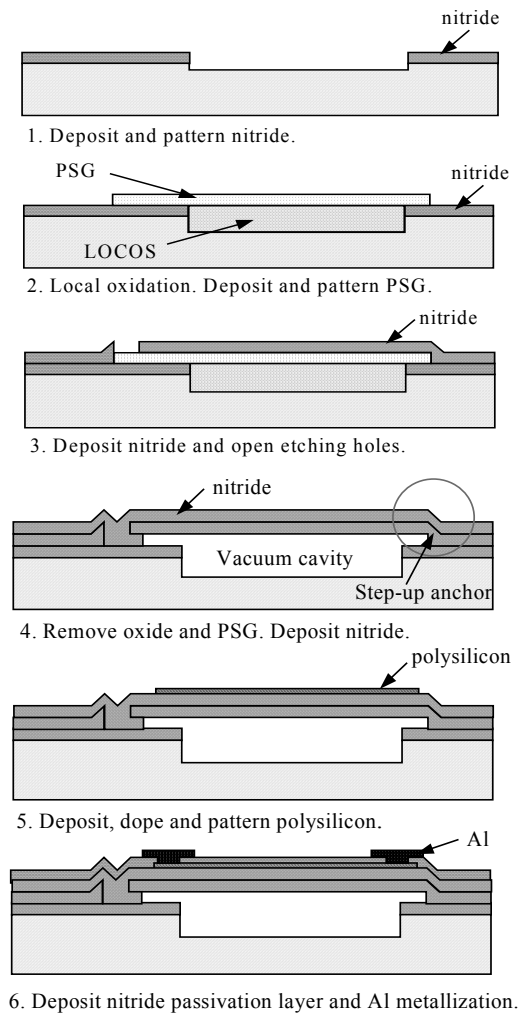
Figure 4 Simplified fabrication process.

As shown in Figure 4, the process starts with the deposition and patterning of low stress silicon nitride on silicon wafers. Windows are etched further into silicon to obtain the desired depth. Thermal oxide is grown locally using LOCOS process on the trench and the wafers are planarized by HF dip. After a 400 nm phosphosilicate glass (PSG) layer is deposited, patterned and annealed to form the etching channels for the cavity, about 1.5 μm of low stress nitride is deposited and patterned to open the etching holes. The PSG and thermal oxide are etched away by 49% HF so that the nitride diaphragms are released. After this, another nitride layer is deposited to reach the desired diaphragm thickness and seal the cavity at the same time. Next, 500 nm polysilicon films are deposited, doped and patterned to form the sensing resistors. Next, another 200 nm nitride is deposited as a passivation layer. After the contact holes

are opened, 1.5 μm aluminum is sputtered, patterned and sintered. Finally the wafer is diced and a 2 μm Parylene C is deposited. Figure 5 shows a fabricated sensor chip with 2 rows of sensors with different diaphragm widths.
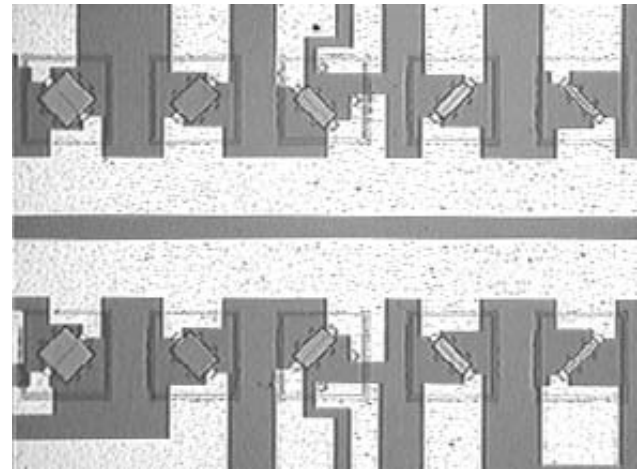

Figure 5 Two rows of sensors with different diaphragm widths.

TESTING AND DISCUSSION

Shown in Figure 6 are the shear-stress calibration data of the four sensors with various diaphragm widths (75μm, 100μm, 150μm and 210μm). Note that the data are normalized to the voltage with zero shear stress. All the sensors operate in constant temperature mode[1] with a working temperature 35 °C above ambient water. As expected, the sensor with larger diaphragm has higher shear-stress sensitivity. The average shear-stress sensitivities are between 0.31 V/Pa and 1.10 V/Pa.

The results of pressure sensitivity measurement of sensors are illustrated in Figure 7. It is observed that the resistance change of the 210 μm sensor is negative and as the diaphragm width decreases, the slope gets closer to zero. The 75 μm sensor exhibits the minimum pressure sensitivity. The 45 μm sensor shows positive resistance change, which is due to the dominance of the transverse strain when W is much smaller than L. The pressure sensitivity shown here is expressed in terms of resistance change. When it is expressed in terms of Volts/psi, the 75 μm sensor exhibits a pressure sensitivity of 5.9 mV/psi.

For a specific application that requires the shear-stress sensor to be operated within 10 feet of water (4.3 psi), the noise caused by the pressure change is 25 mV. Therefore, within 10' of water, the maximum error of the shear-stress reading caused by the pressure sensitivity of the 75 μm sensor is 0.08 Pa (i.e., 25/310=0.08), which is very satisfactory.

---

[1] When in constant temperature mode, the temperature of the shear-stress sensor remains constant during the operation. Refer to [10] more details.

There are many other possible ways to further improve the sensor accuracy besides using the on-chip pressure sensor to do pressure compensation. For example, we can increase the operating temperature of the sensor so that the shear-stress sensitivity will increase while the pressure sensitivity will decrease [10]. However, the operating temperature can not be too high in order to avoid the bubble generation in the water. In terms of fabrication, the sensing element (polysilicon resistor) can be buried in the middle plane of the nitride diaphragm in the cost of making the contact-hole opening process more complicated. Examining Equation (1), it is clear that the gauge factor of polysilicon contributes considerably to the pressure sensitivity. Therefore, it is of great interest to use platinum, whose gauge factor is much smaller, as the heating element.

Also note that Figure 7 only depicts the effect of diaphragm dimension on pressure sensitivity. There is another variable that we can adjust to minimize the pressure sensitivity, which is the resistor length across the diaphragm.
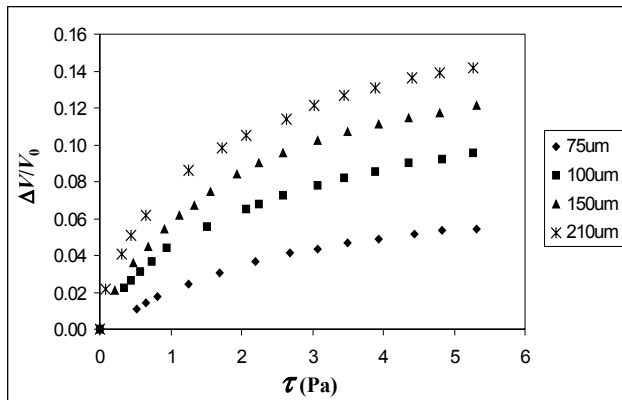

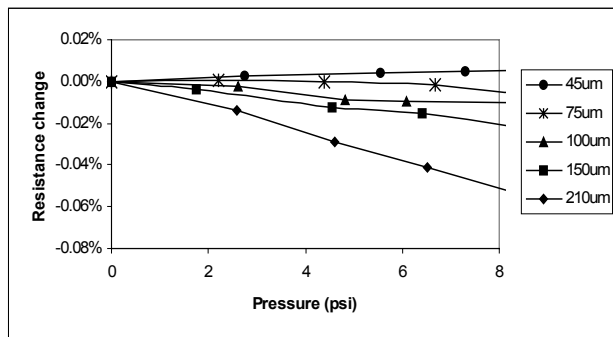Figure 6 Normalized output voltages of four different sensors as functions of shear stress.

Figure 7 The pressure sensitivity of sensors with different diaphragm widths.

CONCLUSION

Micromachined thermal shear-stress sensors for underwater application are successfully fabricated and tested. Parylene is used as the waterproof material and sensors coated with 2 μm Parylene N can survive in water

for at least one month when operated at 55 °C. Adjusting either the diaphragm width or the polysilicon resistor length can minimize the pressure sensitivity. Although it is possible to have zero pressure sensitivity using a large and thin diaphragm, small and thick diaphragm is preferred to achieve a better controllability, higher yield and larger operating range. It is demonstrated that the 75 μm sensor has a maximum shear-stress error of 0.08 Pa for applications within 10 feet of water. There are several ways to further reduce the pressure sensitivity. For example, the operating temperature can be increased, the sensing element can be buried in the middle plane of the nitride diaphragm, or platinum can be employed due to its small gauge factor.

REFERENCES

1. Jiang, F., et al. *Flexible shear stress sensor skin for aerodynamics applications*. in *IEEE International Conference on Micro Electro Mechanical Systems (MEMS)*. 2000. Miyazaki, Japan. p. 364-369
2. Tsao, T., et al., *MEMS-Based Active Drag Reduction in Turbulent Boundary Layers*, in *Microengineering Aerospace Systems*, H. Helvajian, Editor. 1999, The Aerospace Press. p. 553-580.
3. Liu, C., et al. *Surface Micromachined Thermal Shear Stress Sensor*. in *ASME International Mechanical Engineering Congress and Exposition*. 1994. Chicago, IL. p. 9-15
4. Jiang, F., et al. *A Surface-Micromachined Shear Stress Imager*. in *IEEE International Conference on Micro Electro Mechanical Systems (MEMS)*. 1996. San Diego, CA. p. 110-115
5. Schmidt, M.A., et al., *Design and Calibration of a Microfabricated Floating-Element Shear-Stress Sensor*. IEEE Transactions on Electron Devices, 1988. Vol. **35**(6): p. 750-757.
6. Cain, A., et al. *Development of a wafer-bonded, silicon-nitride membrane thermal shear-stress sensor with platinum sensing element*. in *Solid-State Sensor and Actuator Workshop*. 2000. Hilton Head Island, South Carolina. p. 300-303
7. *Parylene Data Sheet*, Specialty Coating System, Indianapolis.
8. Xu, Y., et al. *A Surface Micromachined Nitride-Diaphragm High-Pressure Sensor for Oil Well Application*. in *ASME International Mechanical Engineering Congress and Exposition*. 2000. Orlando, Florida. p. 425-429
9. Wang, C.-T., *Applied Elasticity*. 1953: McGraw-Hill.
10. Xu, Y., et al. *Mass Flowmeter Using a Multi-Sensor Chip*. in *IEEE International Conference on Micro Electro Mechanical Systems (MEMS)*. 2000. Miyazaki, Japan. p. 541-546